Holographic Transmission Gratings for Spectral Dispersion

Introduction

Over the last 12 years, holographic transmission diffraction gratings have been employed within solid-state laser systems to provide angular spectral dispersion (ASD) for laser beam smoothing. The dispersive property of diffraction gratings provides a versatile means to control the spatial and temporal characteristics of high-bandwidth laser light. Recent research has shown that holographic transmission gratings can possess not only high diffraction efficiency and high damage threshold but also high wavefront quality.

In general, spatial or temporal information that is encoded onto a propagating laser beam can be transferred between time and space by means of the lateral time delay associated with a grating's ASD. At LLE, the ASD from a grating is used to carry out laser beam smoothing involving broadband laser operation.[1] At other laser-fusion facilities, holographic diffraction gratings are being developed for broadband frequency conversion to achieve ultra-uniform levels of irradiation uniformity on solid-state laser systems. In addition, several novel pulse compression, pulse expansion, and pulse shaping schemes, involving highly dispersive holographic gratings, have been extensively developed at many laboratories, including LLE.

This article reviews the latest results from our experimental research in holographic-grating fabrication. The performance of recently fabricated holographic gratings is described in terms of diffraction efficiency and wavefront quality. In addition, several important applications of the holographic transmission grating, such as laser beam smoothing on the OMEGA laser system, are reviewed.

Theoretical Modeling

A periodic thickness variation, or surface relief, formed along one dimension of a photosensitive material, such as photoresist, can deflect an incident laser beam by way of diffraction, as shown in Fig. 82.26. A periodic refractive-index variation within a flat film of material can also act as a diffraction grating. Photorefractive polymers have recently been modulated to form efficient gratings; however, this will be the subject of a future article. The type of holographic transmission grating that is based on surface relief of a transparent material diffracts light according to the same diffraction-grating equation as pertains to the volume holograms, reflection gratings, and conventionally ruled gratings. The grating equation

$$d\left[\sin\left(\theta_d\right)-\sin\left(\theta_i\right)\right]=m\lambda \tag{1}$$

is used to calculate the angle of diffraction (θ_d) for a wavelength λ when the angle of incidence (θ_i) of the laser beam and the groove spacing d of the grating are given. This calculation can be performed for any order of diffraction m; however, only the first order of diffraction is important for the majority of applications.

The ASD of the grating is defined as the rate of change of the diffraction angle with respect to change in wavelength. The ASD is a measure of the angular spreading of the spectral components of light and is calculated using Eq. (2):

$$\Gamma = m/d\cdot\cos\left(\theta_d\right). \tag{2}$$

When used in the symmetric-angle configuration, the angle of the incident laser beam is equal to the angle of the primary diffracted beam, i.e., $(\theta_d)=-(\theta_i)$, where the angles are defined with respect to the plane of the photoresist layer. For this symmetric case, where the lateral magnification between the input beam and the output beam is unity, and m represents the first order of diffraction, the expressions for the grating equation and angular dispersion become

$$2d\cdot\sin\left(\theta\right)=\lambda \tag{3}$$

and

$$\Gamma = 2\cdot\tan\left(\theta\right)/\lambda, \tag{4}$$

respectively. These fundamental grating equations are used to design optical systems with a desired amount of ASD.

An optimum grating design couples as much light as possible to the diffracted laser beam. Figure 82.26 also shows the various paths that can be taken by an incident laser beam. The energy coupled to all additional beam paths is minimized to obtain the highest possible diffraction efficiency, defined as the ratio of the powers of the primary diffracted beam to the incident laser beam. However, even small amounts of energy recirculating within the substrate can cause undesirable temporal modulation. In practice, the grating substrate contains a wedge between the first and second surfaces to prevent secondary beams from propagating coincident with the primary diffracted laser beam.

The diffraction characteristics of the gratings, shown in Fig. 82.26, have been the subject of much research. Several rigorous electromagnetic theories,[2] each based on Maxwell's equations with appropriate boundary conditions, are available to calculate the performance of a diffraction grating. Numerical solutions have been obtained for gratings of arbitrary profiles by the integral-equation and differential-equation methods. The integral method[3] is capable of treating both metallic and dielectric gratings and is often used to benchmark further progress in grating modeling. It has been used with limited success, however, in modeling deep multilayered gratings that approach a height-to-width ratio near 2 to 1.

Previously, the differential method involved either an orthogonal-mode expansion or a coupled-wave expansion, each containing a large system of equations that were difficult to manage computationally. An improved differential method, however, involving a nonorthogonal coordinate system, was shown to accurately model deep, multilayered, metal and/or dielectric gratings.[4] Most recently, major enhancements were made to this method to allow transmitted orders as well as reflected orders.[5]

The modeling results shown in this article were obtained with a code based on the integral method. Since our experimental results have sometimes exceeded the predicted values for diffraction efficiency from this code, as will be addressed later in this article, an alternate code based on the more recent differential method will be examined in the near future.

Grating Fabrication

The fabrication of holographic diffraction gratings involves an interferometric exposure of a photosensitive material called photoresist.[6] The holographic interferometer, shown in Fig. 82.27, consists of a laser source, beam-conditioning optics, and two beamlines that intersect at the final recording

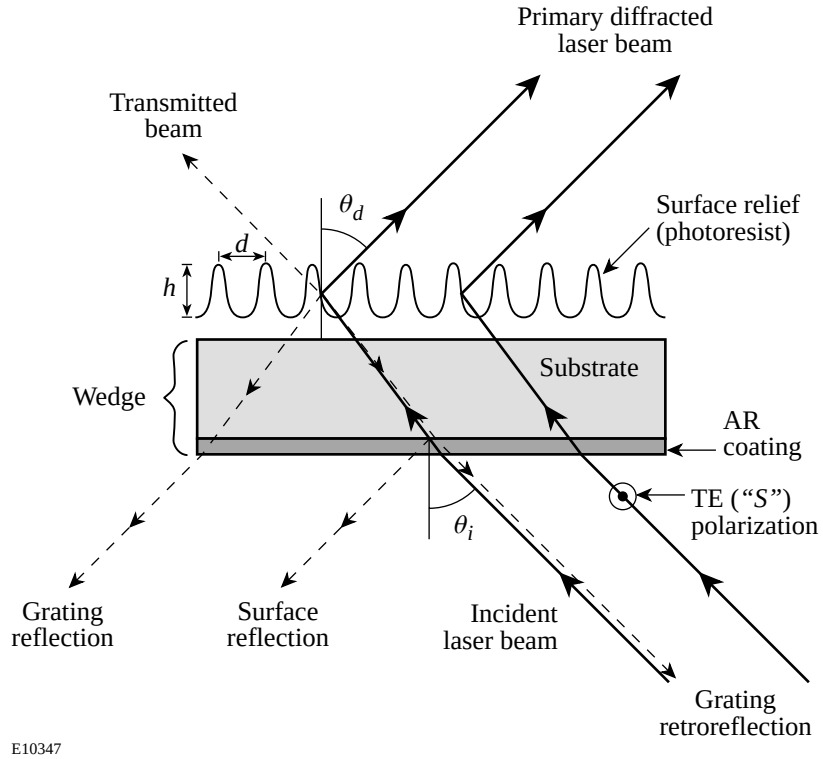

Figure 82.26
A holographic transmission grating, patterned in photoresist, consists of a periodic thickness variation, or surface relief, along one dimension of a material. When used in the symmetric-angle configuration, the angle of the incident laser beam is equal to the angle of the primary diffracted beam, with respect to the plane of the photoresist layer. The energy coupled to all additional beam paths is minimized to obtain the highest-possible diffraction efficiency, defined as the ratio of the powers of the primary diffracted beam to the incident laser beam.

plane. It is used to produce highly visible and stable interference fringes. The laser source is a Spectra-Physics argon-ion laser equipped with an intracavity etalon, narrow-band cavity mirrors, and electronic feedback control to maintain beam power, beam centering, and a single longitudinal mode at the $\lambda = 364$-nm spectral line. Prior to being split into two separate beam paths, the laser beam is raster scanned over the entrance pupils of the two arms of the interferometer. As shown in Fig. 82.28, rotation of a glass cylinder causes a displacement of an incident laser beam without a corresponding change to the laser beam propagation direction. The irradiance at every point within the clear aperture is the superposition of an array of supergaussian beams, resulting in two-dimensional uniformity. This displacement scanning technique increases the exposure uniformity far beyond that of the laser beam itself.[7] With careful chemical processing, fringe exposure results in deep grooves over the entire clear aperture of the grating.

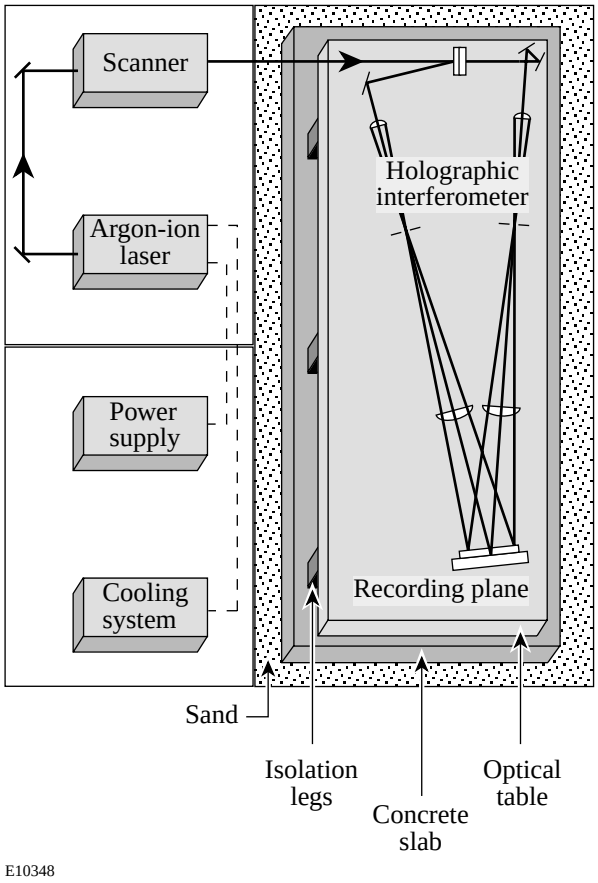

Figure 82.27
The holographic system consists of a laser source, a laser scanner, and an interferometer with two beamlines that intersect at the final recording plane. It produces high-contrast interference fringes. Fringe stability is achieved through a vibration isolation system containing a 2-ft-thick, 8-ft × 16-ft optical table, pneumatically floating on six legs and supported by a 2-ft-thick concrete slab, all resting on a foundation of dry sand. The laser power supply and cooling system, the laser resonator and scanner, and the holographic interferometer are located in three separate rooms to minimize the transfer of vibrations, heat, and atmospheric turbulence.

After exiting the laser scanner, the laser beam is split so that the two arms of the interferometer impose equal amounts of increased path length to an incident beam when the beam is angularly deviated prior to the split. This is the same criterion that was established for the Michelson interferometer,[8] which used an incoherent white-light source. This principle is extended to coherent laser light to achieve stable interference fringes during two-dimensional scanning of the laser beam. To further ensure fringe stability, a 2-ft × 8-ft × 16-ft optical table is pneumatically isolated from building vibrations by six pressurized support legs located on a 2-ft-thick concrete slab. This support system rests on a 3-ft mound of dry sand. To isolate the system from sources of acoustic energy, thermal energy, and air turbulence, the interferometer is located in a "room within a room" environment. Furthermore, the laser power supply and cooling system, the laser resonator and scanner, and the holographic interferometer are located in three separate rooms to minimize the transfer of vibrations, heat, and air turbulence.

In practice, however, it has been found that the holographic system performs optimally only after the room air conditioning has been shut down for between 5 to 20 h, depending on the time of the year. The exact time interval appears to depend on the relationship between the temperature of the ground and the temperature of the air supplied by the building's air-conditioning system. Fringe visibility is continuously monitored prior to a series of holographic exposures. The fringe contrast must remain stable for a period of time exceeding the actual duration of the scan. Otherwise, changes in contrast will map directly to low-efficiency regions of the diffraction grating. Extensive testing has revealed that the success or failure of holographic-grating fabrication does not generally depend on the extent of nearby building or ground activity.

A scanning electron microscope (SEM) is used to characterize the surface relief of the holographic gratings. The size and shape of the grooves are shown in Fig. 82.29. In Fig. 82.29(a), close-up examination of the photoresist surface-relief grating shows a groove shape corresponding to 80% diffraction efficiency, where efficiency is defined as the ratio of the diffracted to incident laser power. Although the surface-

relief profile is not strictly sinusoidal, the etched volume is only slightly larger than the remaining photoresist volume. The SEM in Fig. 82.29(b) shows that the etched volume is much wider than the remaining photoresist volume for a diffraction grating exhibiting over 95% efficiency. The crests of the grooves are straight and rigid when fabricated in controlled laboratory conditions. The SEM in Fig. 82.29(c) reveals the problem associated with uncontrolled humidity in the vicinity of grating fabrication. In the presence of an excessively humid environment, thin walls of photoresist are deformed by capillary attraction from water accumulated within the grooves. It has been observed that groove deformation is accompanied by an increased amount of scatter when probed by a beam of laser light. This is because a distribution of groove deformations acts as a diffuser, scattering light over a broad angular spectrum. Although the mechanical fragility of photoresist structures has long been known, this represents the first time that a specific groove deformation has been associated with the onset

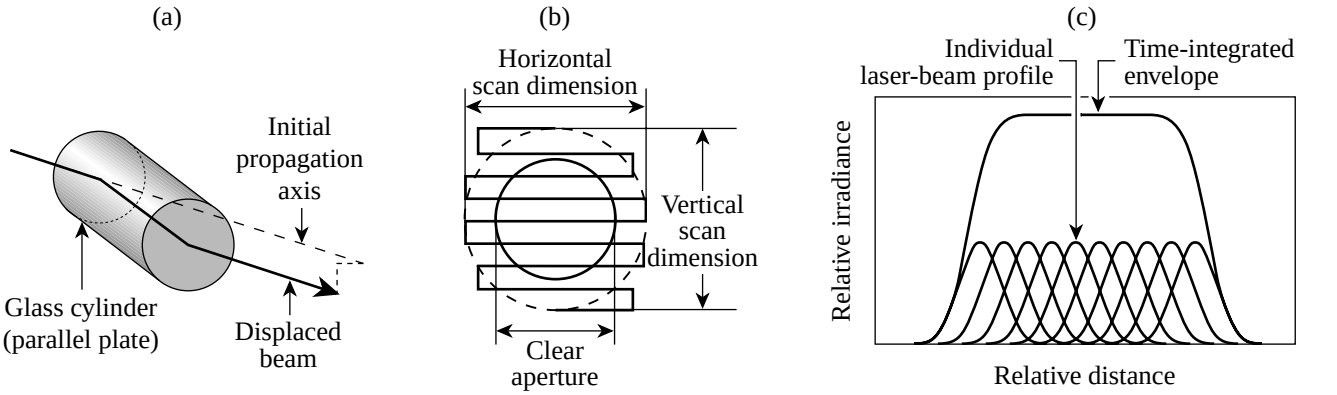

Figure 82.28
Laser-beam scanning is used to increase the time-integrated irradiation uniformity at the recording plane. (a) A tilted glass cylinder displaces an incident laser beam without angular deflection. (b) The laser beam is raster scanned over the entrance pupils of the two arms of the interferometer. (c) The recording-plane irradiance is the superposition of an array of supergaussian beams. The resulting irradiance is substantially more uniform than the laser beam itself.

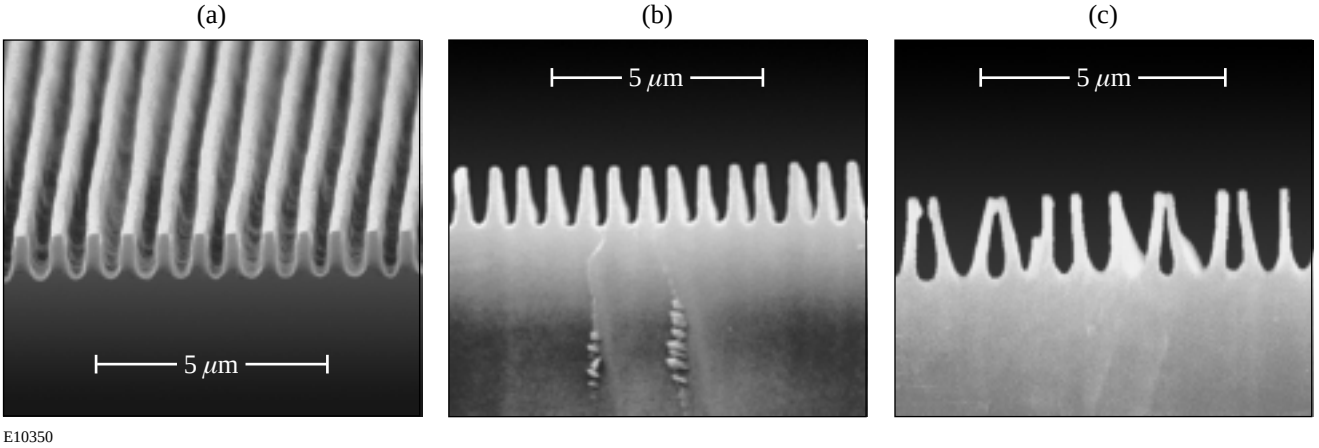

Figure 82.29
The scanning electron microscope (SEM) provides close-up examination of photoresist gratings. Figure 82.29(a) shows the groove profile corresponding to 80% diffraction efficiency, where efficiency is defined as the ratio of the diffracted to incident laser power. Figure 82.29(b) shows that the etched volume is much wider than the remaining photoresist volume for a diffraction grating exhibiting over 95% efficiency. The crests of the grooves are straight and rigid when fabricated in controlled laboratory conditions. The SEM of Fig. 82.29(c) reveals the problem associated with uncontrolled humidity in the vicinity of grating fabrication. Thin walls of photoresist are deformed by capillary attraction from water accumulated within the grooves. Groove deformation is accompanied by an increased amount of laser light scatter.

of scatter loss. As a result of this understanding, careful washing and drying procedures are used to fabricate super-sinusoidal groove shapes.

Grating Performance

Holographic transmission gratings possess deep grooves that, when properly shaped, result in near-unity diffraction efficiency for a wide range of groove spacing. Within the holography laboratory at LLE, transmission gratings have been designed and fabricated for use at three different symmetric angles. At the symmetric angle, the incident and diffracted beams have equal angles with respect to the normal to the grating. Theoretical calculations of the diffraction efficiency, shown in Fig. 82.30, predict that performance decreases for gratings with larger groove spacing, i.e., a smaller symmetric angle. Experimental results for these three different symmetric angles indicate, however, that diffraction efficiency can be maintained at a level higher than the integral-equation method predicts. Experimental results for symmetric angles (groove spacings) of 31.7° (1.00 μm), 46° (0.73 μm), and 49.5° (0.69 μm) show that high diffraction efficiency is possible over this entire range of angles.

Theoretical and experimental results show that a super-sinusoidal phase grating can exhibit high efficiency. As shown in Fig. 82.31, the diffraction efficiency of a super-sinusoidal phase grating decreases slowly and monotonically as it is detuned in angle. This curve represents a grating designed for a symmetric angle of 46°; however, similar performance is obtained for a wide range of angles. As shown in Fig. 82.32, it has been observed that holographic gratings with larger groove spacing, such as the 31.7° grating, exhibit an efficiency profile that drops rapidly at several specific angles when detuned from

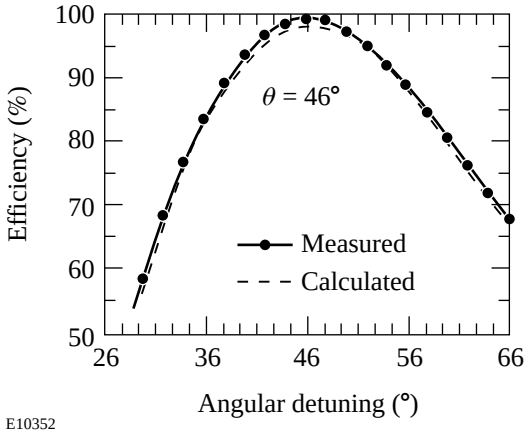

Figure 82.31
Theoretical and experimental results show that the diffraction efficiency of a typical surface-relief transmission grating decreases slowly and monotonically as it is detuned in angle about the peak efficiency, where the incident and diffracted angles are equal. The curves represent a grating designed for a symmetric angle equaling 46°; however, similar performance is obtained for a wide range of angles.

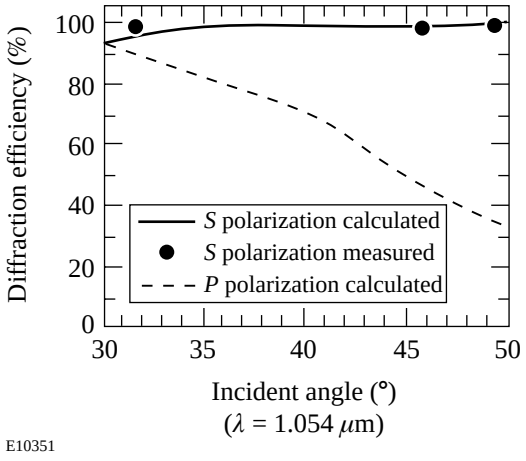

Figure 82.30
Holographic transmission gratings possess deep grooves that, when properly shaped, result in near-unity diffraction efficiency for a wide range of groove spacing. Theoretical calculations of the diffraction efficiency predict that performance decreases for gratings with a symmetric angle decreasing toward 30°. Experimental results for symmetric angles (groove spacings) of 31.7° (1.00 μm), 46° (0.73 μm), and 49.5° (0.69 μm) show that diffraction efficiency can be maintained over this whole range of angles.

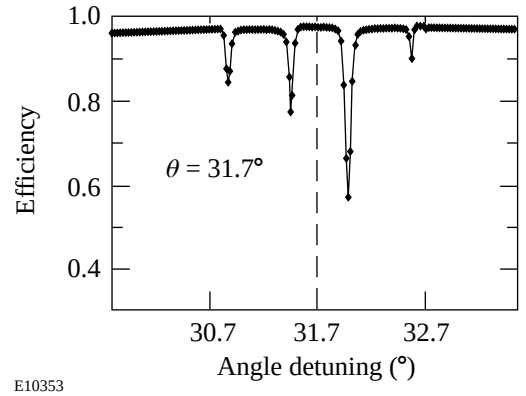

Figure 82.32
Holographic gratings with larger groove spacing, such as the 31.7° grating, exhibit an efficiency profile that rapidly drops at several specific angles when detuned from the symmetric angle. Except for these narrow regions in angle, the measured diffraction efficiency exceeds theoretical predictions. It is observed that the thickness of the photoresist affects the extent to which laser light travels within the photoresist waveguide before being coupled out along the $m = -1$ diffraction order.

the symmetric angle. Except for these narrow regions in angle, the measured efficiency exceeds theoretical predictions. A preliminary investigation of this effect revealed that the thickness of the photoresist affects the extent to which laser light propagates down the photoresist waveguide before being coupled out along the first diffraction order. This waveguide-coupling phenomenon has been correlated to the rapid efficiency drop at specific angles. Additional experimental investigation is needed to determine the maximum photoresist thickness allowed before waveguide modes can exist. It has been experimentally determined that efficient use of the 31.7° grating within the OMEGA laser system requires that an alignment error of less than 10 min of arc be maintained between the laser beam and the grating.

Gratings used within the OMEGA laser *must* possess high optical quality, including both high phase-front quality and minimum phase noise. Holographic phase-front errors, due to optical aberrations within the interferometer, can be measured by analyzing interferograms from both the diffracted beam (minus one order) and the transmitted beam (zero order), individually. The wavefront quality of the diffracted beam, however, is what is important for most applications. Better than one-tenth wave performance is achieved over the clear aperture of a grating used for the OMEGA laser system, as shown in Fig. 82.33(a). Cross sections of the wavefront error are shown in Fig. 82.33(b). This error originates from the two telescopes within the interferometer. The difference in curvature between the two cross sections indicates the presence of astigmatism, the aberration which causes the tangential (horizontal) and sagittal (vertical) planes to focus at different planes. In practice, interferometer alignment is repeated until the measured wavefront error is minimized. In addition, small-scale imperfections are reduced by using high-quality optics and coatings within the interferometer, and by carrying out the photoresist deposition in a well-maintained clean-room laboratory.

Laser Applications

The primary applications of holographic diffraction gratings at LLE involve laser-beam smoothing and spectroscopy. Several sets of gratings, with angular dispersions of between 120 to 220 μrad per angstrom, are now available for one of OMEGA's driver lines for the purpose of laser beam smoothing. Also, high-resolution spectrometers, composed of one or more holographic gratings, are used to characterize the modulation index of phase modulators for broadband beam smoothing. In addition, it is possible that two large-aperture gratings, used in series with a focusing lens, can provide sufficient ASD to fully resolve the individual line structure from a sinusoidally driven modulator. It is important to note that by having holographic gratings incorporated into the driver line of OMEGA, each of the OMEGA beamlines is a potential spectrometer for diagnosis of the laser bandwidth.

A wide variety of additional applications exist for high-efficiency, high-damage-threshold, holographic diffraction gratings. For example, holographic gratings can be used to carry out broadband frequency conversion to achieve ultra-uniform levels of irradiation uniformity on solid-state laser

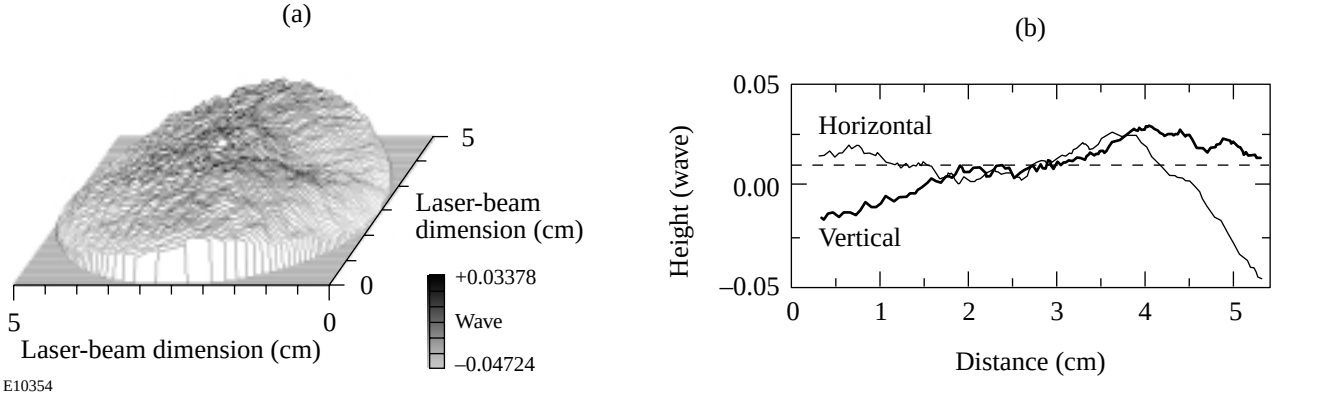

Figure 82.33
(a) Better than one-tenth wave performance is achieved over the clear aperture of a 31.7° grating used in the OMEGA laser system. (b) Cross sections of the wavefront indicate that the largest low-frequency aberration is astigmatism. This error originates from the two telescopes within the interferometer. High-quality optics and mounts can provide similar wavefront quality for large-aperture gratings.

systems. In addition, several novel pulse-compression and pulse-expansion schemes include holographic gratings in their optical design. Advanced pulse-shaping schemes also involve highly dispersive holographic gratings, which provide compactness, high damage threshold, and high diffraction efficiency. Holographic transmission gratings are used within compact spectrometers, fiber-optic couplers, laser scanners, and various semiconductor lasers. Additional applications of high-power, high-dispersion transmission gratings involve their function as a spectral filter. These gratings provide excellent Fourier-blocking capability for small-signal-gain detection and for the suppression of amplified stimulated emission in amplifier chains. It is anticipated that many new applications will be found for holographic transmission gratings when the gratings become more widely available.

Conclusion

Holographic transmission gratings that possess high diffraction efficiency, high wavefront quality, and high damage threshold have been designed, fabricated, and characterized for use within high-power, solid-state laser systems. Holography research has resulted in diffraction gratings that exhibit near-unity efficiency over a wide range of groove spacing. A novel interferometric technique that incorporates laser beam scanning is now routinely used to obtain uniform grating irradiation while maintaining stable, high-contrast, interference fringes. Over 100 gratings, covering a wide range of groove spacing, have been manufactured with this interferometric exposure technique. Several sets of gratings, with different amounts of angular dispersion, are available for one of the driver lines of the OMEGA laser. Numerous applications exist for these high-efficiency, high-damage-threshold holographic gratings. Laser beam smoothing and spectroscopic techniques, many of which have been invented and developed at LLE, incorporate these gratings. High-efficiency and high-wavefront-quality gratings are now in use within the beam-smoothing driver line of the OMEGA laser system. The current research thrust involves an experimental and theoretical investigation of the gratings that exhibit diffraction efficiency that exceeds code predictions and also exhibit waveguide coupling of laser light.

ACKNOWLEDGMENT

This work was supported by the U.S. Department of Energy Office of Inertial Confinement Fusion under Cooperative Agreement No. DE-FC03-92SF19460, the University of Rochester, and the New York State Energy Research and Development Authority. The support of DOE does not constitute an endorsement by DOE of the views expressed in this article.

REFERENCES:

1. Laboratory for Laser Energetics LLE Review **37**, 40, NTIS document No. DOE/DP/40200-83 (1988). Copies may be obtained from the National Technical Information Service, Springfield, VA 22161.
2. R. Petit, ed. *A Tutorial Introduction*, Electromagnetic Theory of Gratings (Springer-Verlag, Berlin, 1980).
3. D. Maystre, J. Opt. Soc. Am. **68**, 490 (1978).
4. J. Chandezon *et al.*, J. Opt. Soc. Am. **72**, 839 (1982).
5. L. Li, "DELTA: A Computer Program for Multilayer-Coated Gratings in Conical Mountings," computer manual (1999).
6. Laboratory for Laser Energetics LLE Review **50**, 61, NTIS document No. DOE/DP/40200-197 (1992). Copies may be obtained from the National Technical Information Service, Springfield, VA 22161.
7. J. J. Armstrong and T. J. Kessler, in *Laser Coherence Control: Technology and Applications*, edited by H. T. Powell and T. J. Kessler (SPIE, Bellingham, WA, 1993), Vol. 1870, pp. 47–52.
8. A. A. Michelson, Am. J. Sci. **22**, 120 (1881).